

# TITANIUM DIOXIDE SOL-GEL/ZINC OXIDE POWDER-COATED CLAY BEADS IN PHOTOCATALYTIC REACTOR

## Article history

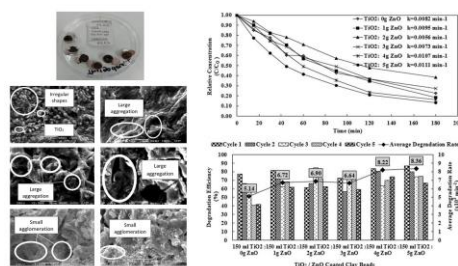
Received  
27 March 2022  
Received in revised form  
5 October 2022  
Accepted  
13 October 2022  
Published Online  
26 December 2022

Thurgadewi Krishnan, Ng Con Nie, Wan Rafizah Wan Abdullah, Mohamad Awang, Wan Salida Wan Mansor\*

Faculty of Ocean Engineering Technology and Informatics, Universiti Malaysia Terengganu, 21030 Kuala Nerus, Terengganu, Malaysia

\*Corresponding author  
wansalida@umt.edu.my

## Graphical abstract



## Abstract

Catalyst Immobilization methods are important for providing better recovery of catalyst in photocatalytic treatment. The aim is to characterize and evaluate the photocatalytic performance of TiO<sub>2</sub>/ZnO-coated clay beads. The titanium dioxide/zinc oxide (TiO<sub>2</sub>/ZnO)-coated clay beads were prepared via the sol-gel process. Various ZnO powder ratios gave different TiO<sub>2</sub>/ZnO composites sol. Four layers of TiO<sub>2</sub>/ZnO sol were coated on clay beads and dried in the oven at 100°C for 30 min. The coated clay beads were calcined at 500°C for one hour for every two layers. Characterization of coated clay beads was done using a scanning electron microscope and energy dispersive spectroscopy. The increased surface area on small agglomeration and optimum loading of ZnO (5 g) resulted in the highest degradation efficiency recorded at 86.57%. An effective catalyst immobilization achieved a good recycling performance on clay beads. Degradation rate data were presented by pseudo-first-order kinetics. It was observed that the average degradation rate for TiO<sub>2</sub>/5 g ZnO is 0.00836 min<sup>-1</sup>. The actual results in this work can be applied as a guideline for the preparation of TiO<sub>2</sub>/ZnO-coated clay beads with high photocatalytic performance.

**Keywords:** TiO<sub>2</sub>/ZnO clay beads, sol-gel, photocatalysis, degradation rate, beads recyclability

## Abstrak

Kaedah imobilisasi pemangkin adalah penting untuk menyediakan cara pemulihan pemangkin yang lebih baik dalam rawatan fotomangkin. Matlamat kajian ini adalah untuk mencirikan dan menilai prestasi fotopemangkin bagi manik tanah liat bersalut TiO<sub>2</sub>/ZnO. Manik tanah liat bersalut titanium dioksida/zink oksida telah disediakan melalui kaedah 'sol-gel'. Nisbah serbuk ZnO yang berbeza telah memberikan sol komposit TiO<sub>2</sub>/ZnO yang berbeza. Empat lapisan sol TiO<sub>2</sub>/ZnO telah disalutkan pada manik tanah liat dan dikeringkan dalam ketuhar pada suhu 100°C selama 30 minit. Manik tanah liat yang bersalut telah dikalsinasi pada 500°C selama satu jam bagi setiap dua lapisan. Pencirian manik tanah liat bersalut telah dilakukan menggunakan 'scanning electron microscope dan 'energy dispersive spectroscopy'. Pertambahan luas permukaan pada penggumpalan kecil dan pemuatan optimum ZnO (5 g) telah menghasilkan kecekapan degradasi tertinggi dicatatkan pada 86.57%. Kaedah imobilisasi pemangkin yang berkesan telah mencapai prestasi kitar semula yang baik pada manik tanah liat. Data kadar degradasi telah menunjukkan mengikut kinetik tertib pertama. Diperhatikan bahawa purata kadar degradasi untuk TiO<sub>2</sub>/5 g ZnO adalah

0.00836 min<sup>-1</sup>. Hasil sebenar dalam kajian ini boleh diaplikasikan sebagai panduan bagi penyediaan manik tanah liat bersalut TiO<sub>2</sub>/ZnO yang memberikan prestasi fotomangkin yang terbaik.

**Kata kunci:** Manik tanah liat TiO<sub>2</sub>/ZnO, *sol-gel*, fotomangkin, kadar degradasi, kebolehkitar semula manik

© 2023 Penerbit UTM Press. All rights reserved

## 1.0 INTRODUCTION

Semiconductor nanocomposites provide high interest in photocatalytic applications because of their improved properties [1, 2]. Titanium dioxide (TiO<sub>2</sub>), a semiconductor from abundantly available metal, has been investigated as one of the most promising photocatalyst candidates due to its non-toxicity, cheapness, and highly reactive properties [3, 4]. Applications of TiO<sub>2</sub> in environmental remediation relating to wastewater treatment, air purification, and disinfection were also observed [5]. For instance, Hachem *et al.* (2001) reported that textile dyes decolourisation performed by commercial Degussa P25 TiO<sub>2</sub> using homemade reactor under 18 W UV fluorescent lamp irradiation [6]. In a recent study, methylene blue degradation was executed by flowerlike rutile phase TiO<sub>2</sub> film on a photocatalytic reactor under a 300 W xenon lamp [7]. Moreover, Zinc oxide (ZnO) also has a comparable band gap with TiO<sub>2</sub>, making it an equally efficient photocatalyst [8]. In 1994, kraft black liquor effluent from the paper and pulp industry was treated with a 250 W mercury lamp by commercial ZnO catalyst [9]. Recently, photocatalytic degradation of phenol was performed by fabricated ZnO nanorods under 1000 W/m<sup>2</sup> solar simulator [10]. ZnO offers a great photocatalytic activity even in small quantities [11, 12]. The similarity indicates the suitability of ZnO to be coupled with TiO<sub>2</sub>.

The coupling of two photocatalysts has become a new method for enhancing photocatalytic activity [13, 14]. The semiconducting material absorbs the light energy and becomes an excited state that further produces a pair of electrons and holes (e<sup>-</sup>/h<sup>+</sup>). The holes (h<sup>+</sup>) produced is a potent oxidizing agent that will react with a water molecule (H<sub>2</sub>O) to create super reactive hydroxyl radicals (HO•) [15]. These hydroxyl radicals will react with dyes or organic pollutants and decompose them into smaller intermediates, such as carbon dioxide (CO<sub>2</sub>) and water (H<sub>2</sub>O) [16, 17]. Several methods have been executed for coupling of these photocatalysts, such as hydrothermal [18], solvothermal [19], spray pyrolysis [20], chemical vapor deposition [21], electrodeposition [22, 23], magnetron sputtering [24], sol-gel [25, 26], and incipient wet impregnation [27]. Among these above-mentioned methods, the sol-gel method is a cost-effective practice with low-temperature synthesis [28-30].

Moreover, photocatalytic treatment has a problem in recovering and recycling powdered catalysts from treated effluent in slurry reactors [31, 32]. Alternatively, catalyst immobilization into solid support material will solve the problem of recovery and recycling of the catalyst. Meanwhile, several studies used quartz glass [33], zeolites [34], chitosan gel beads [35], polymeric beads [36], and clay beads [37]. Few studies have been done on TiO<sub>2</sub>/ZnO-coated clay beads. In Bel Hadjitaief *et al.* research, tunisian clay supported ZnO-TiO<sub>2</sub> were used to assess photocatalytic degradation of methyl green under 100 W UV lamp [38]. Vaizogullar *et al.* was used TiO<sub>2</sub>/ZnO-supported on sepiolite clay for the photocatalytic degradation of flumequine antibiotic under a 2mW/cm<sup>2</sup> spectro line UV lamp [39]. In addition, methylene blue photocatalytic degradation performance was conducted by synthesis of rectorite clay-based ZnO and TiO<sub>2</sub> under simulated sunlight irradiation [40]. The advantages of clay beads over other supporting materials are their vast availability in nature, cheapness, and environmentally friendly [41]. Furthermore, their high porosity is useful, making them great adsorbents [42, 43]. Therefore, the present work aims to characterize and evaluate the photocatalytic performance of TiO<sub>2</sub>/ZnO-coated on clay beads.

## 2.0 METHODOLOGY

### 2.1 Preparation of TiO<sub>2</sub>/ZnO Composites Sol

In the current study, TiO<sub>2</sub>/ZnO composites sol were prepared by directly mixing ZnO powder into TiO<sub>2</sub> sol-gel, synthesized by the sol-gel process. Titanium isopropoxide (Sigma-Aldrich India, 97% v/v) was used to prepare transparent TiO<sub>2</sub> sol at room temperature. Firstly, 101ml of titanium isopropoxide was dissolved in 208ml of 2-propanol (R&M Chemical India, 99.5% v/v). The solution was under continuous stirring by a magnetic stirrer for 2 hours to acquire a precursor solution. Then, a combination of distilled water (7 ml), and acetic acid (1 ml) (R&M Chemical India, ≥99.7% v/v) was dropped into the precursor solution at a speed of 1 drop/s under vigorous stirring. Next, the solution was continuously stirred for 10 min to attain a yellow transparent sol. Then, 105 ml of triethanolamine (Sigma-Aldrich Germany, 99% v/v) was added and stirred for 30 min to increase the

mixture's stability. Subsequently, various amounts of ZnO powder (Aldrich USA, <100 nm particle size w/w) were mixed with a fixed volume of 150 ml TiO<sub>2</sub> sol to form different mass ratios of ZnO (1 g/L, 2 g/L, 3 g/L, 4 g/L, and 5 g/L).

## 2.2 Catalyst Immobilization

The TiO<sub>2</sub>/ZnO-coated clay beads were prepared by the dip-coating method. Before the coating procedure, the clay beads, also known as lightweight expanded clay aggregate (LECA), were washed a few times with water (1000 ml) and acetone (20 ml) for 10 min before being dried in the oven. The clean clay beads were immersed in TiO<sub>2</sub>/ZnO sol at a speed of 1 mm/s. The dip-coated beads were allowed to air dry for 5 min in the fume-hood. Then, those coated clay beads were shifted to an oven at 100°C for 30 min. This process was repeated before the beads moved to a furnace for calcination. The ramp-up heating rate was 2°C/min, and the temperature was held at 500°C for 1 hour before cooling down naturally to minimize cracking. The procedure was repeated to acquire four TiO<sub>2</sub>/ZnO layers, with calcination every two layers.

## 2.3 Characterization of TiO<sub>2</sub>/ZnO-coated Clay Beads

Analytical Scanning Electron Microscopy (SEM) (model: JSM-6360 LA; JEOL) was used to observe the bare and TiO<sub>2</sub>/ZnO-coated clay beads surface morphology. Before SEM imaging, samples were sputter-coated with a gold layer (JFC-1600 Auto fine coater). The surface elemental composition of the samples was determined via Energy Dispersive Spectroscopy (EDS) attached to the SEM. An acceleration voltage of 20.0 kV was applied for imaging for all samples.

## 2.4 Photocatalytic Experiment

Photocatalytic experiments were carried out in a column-shaped glass reactor with a 500-ml capacity. A 13 W UV lamp (WK-X2) was applied as a light source. It was placed vertically inside the reactor (Figure 1). The photocatalytic decolorization experiments were carried out at a known amount of TiO<sub>2</sub>/ZnO-coated clay beads with 500 ml of methylene blue (MB) solution. All mixtures were agitated at 1500 rpm using a magnetic stirrer at room temperature. The effect of varying TiO<sub>2</sub>/ZnO-coated clay beads was carried out in the range of 1 g to 5 g of ZnO mass ratios.

Meanwhile, TiO<sub>2</sub> sol volume was used with a fixed volume. During 180 min reaction time, samples were taken at certain time intervals from the reactor. Those samples were observed with spectrophotometric analysis using UV-Vis spectrophotometry (UV-1800; Shimadzu). The experiments were conducted under degradation kinetics and efficiency studies. The degradation rate follows Langmuir pseudo-first-order kinetics [44, 45] was calculated by the following equation:

$$\ln(C/C_0) = -k \times t \quad (1)$$

The degradation efficiency was calculated as follows:

$$\% \text{ Degradation efficiency} = [C_0 - C_t]/C_0 \times 100\% \quad (2)$$

where,  $k$  is the pseudo-first-rate kinetic constant,  $C_0$  is the initial concentration, and  $C$  is the concentration after the methylene blue degradation for time ( $t$ ).

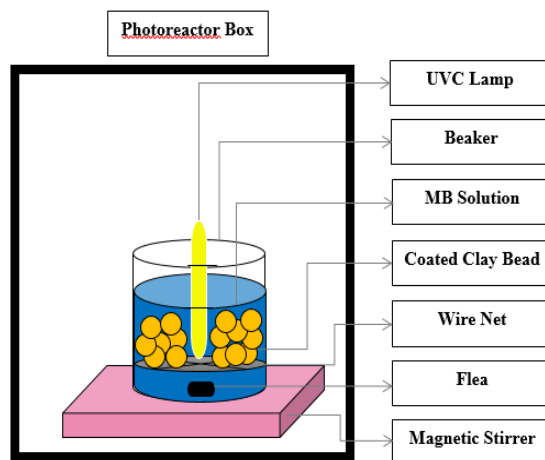


**Figure 1** Experimental setup of photoreactor for photocatalytic experiments

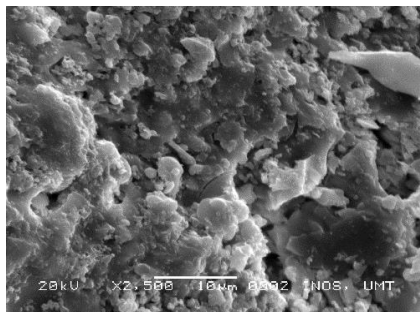
## 3.0 RESULTS AND DISCUSSION

### 3.1 Scanning Electron Microscopy (SEM) Images of TiO<sub>2</sub>/ZnO-coated Clay Beads

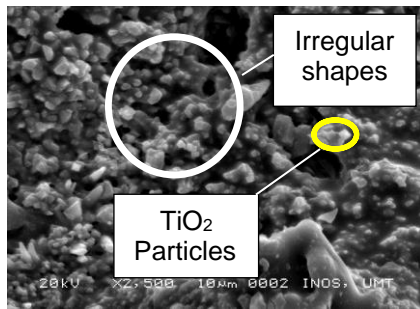
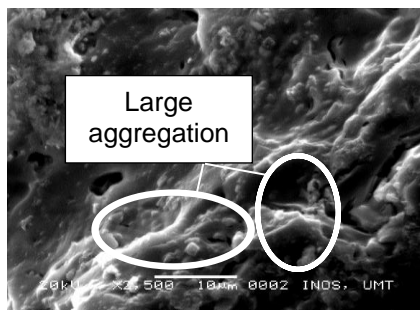
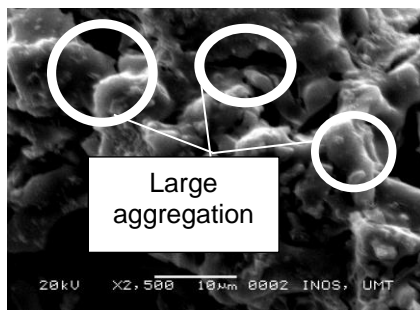
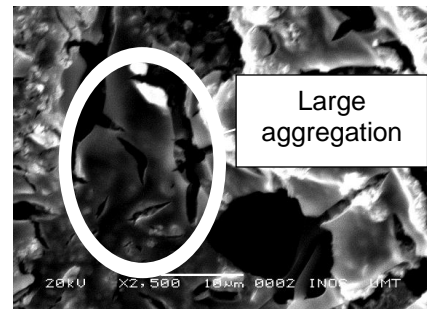
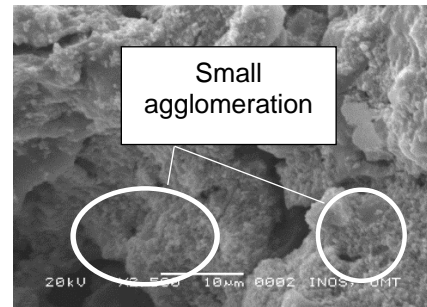
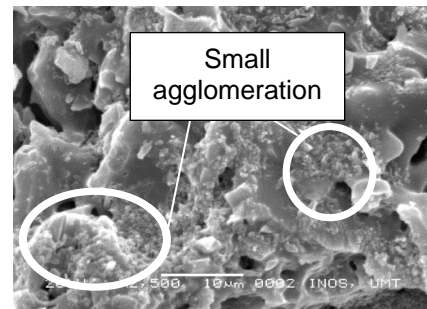
Surface morphology analysis of the bare clay bead and TiO<sub>2</sub>/ZnO-coated clay beads at 2500× magnification was performed, and the results are shown in Figure 2. The SEM image of Figure 2(a) indicates the surface morphology of bare clay beads as compared to that of TiO<sub>2</sub>/ZnO-coated clay beads (Figures 2(b–g)). The surface of the bare clay bead has smooth surfaces with irregular morphological shapes (Figure 2(a)). Figures 2(b–g) are micrographs of coated clay beads that show dispersed TiO<sub>2</sub> and TiO<sub>2</sub>/ZnO nanocomposites on the surface of the clay beads. After the accumulation of nanoparticles, the bare bead morphology modification indicated that the active species (TiO<sub>2</sub> and ZnO) were uniformly scattered on the bead surface [46].

Figure 2(b) reveals TiO<sub>2</sub> nanoparticles synthesized from titanium isopropoxide hydrolysis without adding any ZnO powder. It can be seen that pure TiO<sub>2</sub> nanoparticles aggregates in irregular cubic shapes, where triethanolamine was utilized as a stabilizer which acts as a shape controller [47, 48]. The aggregation could be formed due to the high viscosity of the sol-gel, thus minimizing the dispersion of particles [49]. Figures 2(c–g) exhibit the TiO<sub>2</sub>/ZnO nanocomposite at different mass ratios of ZnO powder. TiO<sub>2</sub> nanoparticles morphology was

affected by ZnO addition [50], and the size of distribution of  $\text{TiO}_2/\text{ZnO}$  nanocomposites was improved in Figures 2(f–g).  $\text{TiO}_2/\text{ZnO}$  nanocomposites have regular morphology comprised of small agglomerates and nanoparticles. It displays a well-ordered structure and good particle distribution [51]. Figures 2(c–e),  $\text{TiO}_2/\text{ZnO}$  nanocomposites reveal some large aggregation with different particle size dispersion. Other work reported that the particle size distribution and agglomeration level appeared to be determined by the  $\text{TiO}_2/\text{ZnO}$  ratio [52].



(a) bare beads

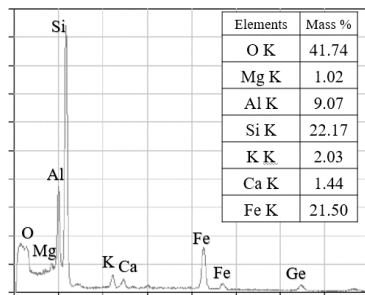
(b)  $\text{TiO}_2$  only(c)  $\text{TiO}_2/1$  g ZnO(d)  $\text{TiO}_2/2$  g ZnO(e)  $\text{TiO}_2/3$  g ZnO(f)  $\text{TiO}_2/4$  g ZnO(g)  $\text{TiO}_2/5$  g ZnO

**Figure 2** SEM micrographs of the bare and  $\text{TiO}_2/\text{ZnO}$  coated clay beads

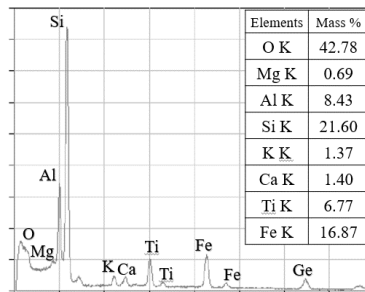
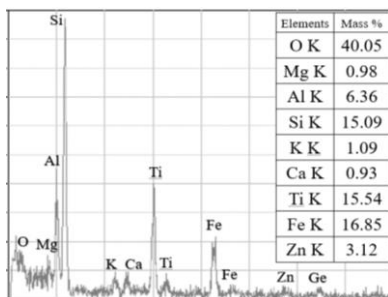
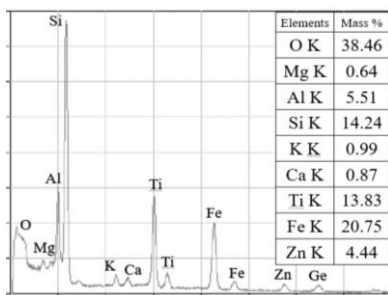
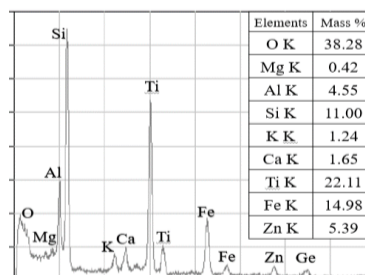
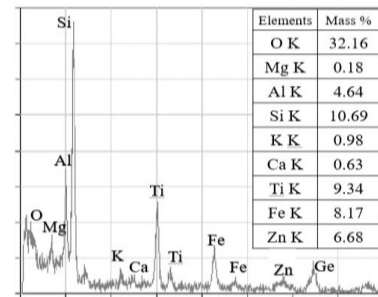
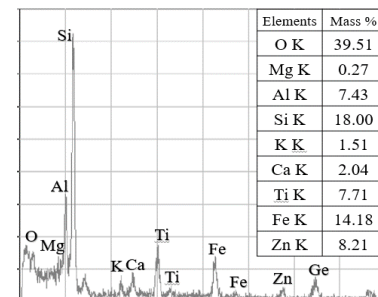
### 3.2 Energy Dispersive Spectroscopy (EDS) Analysis of $\text{TiO}_2/\text{ZnO}$ -coated Clay Beads

Figure 3 shows the energy dispersive spectroscopy (EDS) of bare clay bead and  $\text{TiO}_2/\text{ZnO}$ -coated clay beads with the elemental composition of composites [53]. Presence of elements of oxygen (O), magnesium (Mg), aluminum (Al), silicon (Si), potassium (K), calcium (Ca), and iron (Fe) were detected in clay beads (Figure 3(a–g)). These elements were obtained from the clay beads. Figure 3(b–g) shows the energy dispersion spectra of  $\text{TiO}_2/\text{ZnO}$  composite nanoparticles on clay beads at different ZnO mass ratios. The nanocomposites were mainly composed of Ti, Zn, and O elements. Another study demonstrated that pure  $\text{TiO}_2$  has titanium (Ti) and oxygen (O) signals, but the  $\text{TiO}_2/\text{ZnO}$  nanocomposite has an additional indication of zinc (Zn). This composition indicated that ZnO was successfully incorporated into  $\text{TiO}_2$  nanoparticles to entrap into clay beads [54]. The composition of the

Zn element increases with an increase in ZnO mass ratio.



(a) bare beads

(b) TiO<sub>2</sub> only(c) TiO<sub>2</sub>/1 g ZnO(d) TiO<sub>2</sub>/2 g ZnO(e) TiO<sub>2</sub>/3 g ZnO(f) TiO<sub>2</sub>/4 g ZnO(g) TiO<sub>2</sub>/5 g ZnO

**Figure 3** EDS analysis of the bare and TiO<sub>2</sub>/ZnO coated clay beads

### 3.3 Photocatalytic Properties of TiO<sub>2</sub>/ZnO-coated Clay Beads

The ZnO mass ratio is the parameter that indicates the performance of photocatalytic degradation. Figure 4 shows the effect of the ZnO mass ratio on photocatalytic degradation of MB (25 mg/l) in water under UV irradiation in a batch reactor at different time intervals. The displayed k-values in Figure 4 are from fitting curves of the data for a 0–180 min period. These values represent a valid measurement of all the TiO<sub>2</sub>/ZnO-coated clay beads' photocatalytic degradation rates. TiO<sub>2</sub>/2 g ZnO showed the lowest photocatalytic activity with  $k = 0.0056 \text{ min}^{-1}$ . Moradi *et al.* mentioned that the large aggregation of nanocomposites decreased photocatalytic degradation activity [55]. Meanwhile, TiO<sub>2</sub>/5 g ZnO, with  $k = 0.0111 \text{ min}^{-1}$ , has the fastest MB degradation rate, respectively. More active sites are available in small aggregation due to increased surface area at a higher mass ratio of ZnO than lower mass ratio, which enhance photocatalytic degradation [56].

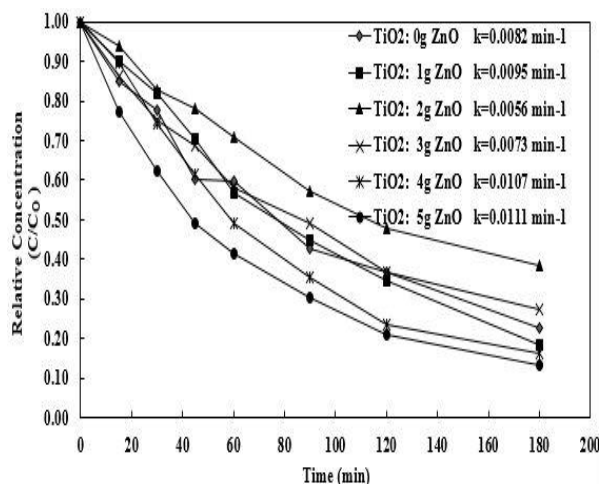


**Figure 4** Photocatalytic degradation of MB under UVC irradiation by TiO<sub>2</sub>/ZnO-coated clay beads.

### 3.4 Recycling Performance of TiO<sub>2</sub>/ZnO-coated Clay Beads

Beads recycling was performed under UV light using a batch photocatalytic reactor with varying TiO<sub>2</sub>/ZnO-coated clay beads for treating 25 mg/l MB solution at a time to evaluate photocatalyst regeneration performances [57]. Figure 5 shows that about five cycles were performed in three hours each, with the highest and lowest degradation efficiency of MB in the 1st and 5th cycles by TiO<sub>2</sub>/5 g ZnO-coated clay beads at 86.57% and 66.81%, respectively; this results in the highest average degradation efficiency of 76.48%.

Moreover, in the literature experimental observation [40], 0.7 g/L of rectorite clay/ZnO/TiO<sub>2</sub> (2:1:0.067) recycling performance was maintained at higher than 60% for five repetitive experiments in photocatalytic degradation of 5 mg/L methylene blue. In another literature experimental observation [38], the recycling performance of 0.8 g/L ZnO-TiO<sub>2</sub>/Tunisian clay photocatalyst was maintained at higher than 95% degradation efficiency for five consecutive cycles in treatment of 75 mg/L of methyl green. In this study, the average MB degradation rate for the TiO<sub>2</sub>/5 g ZnO was calculated to be 0.00836 min<sup>-1</sup>, which portrays an increase in ZnO content incorporated with TiO<sub>2</sub> increases recycling performance [58].

TiO<sub>2</sub>/4 g ZnO-coated clay beads showed a slight decrease in the MB degradation efficiency from Cycle 1 to Cycle 3, but it remained higher than 60% for five cycles with an average degradation rate of 0.00822 min<sup>-1</sup>. On the other hand, recyclability of TiO<sub>2</sub>/ZnO-coated beads with the mass ratio of 1 g to 3 g ZnO displayed the same trend in the average degradation rate (0.00672 min<sup>-1</sup>, 0.00690 min<sup>-1</sup>, and 0.00664 min<sup>-1</sup>), respectively. TiO<sub>2</sub>/ZnO-coated beads without any ZnO powder showed the lowest average MB degradation efficiency, 57.97%, for five cycles with  $k = 0.00514 \text{ min}^{-1}$  because less active sites are

available in TiO<sub>2</sub> only-coated clay beads, causing a lower percentage of MB degradation [59]. Moreover, cubic TiO<sub>2</sub> has lower energy of binding that specifies a less oxidizing state than anatase TiO<sub>2</sub> [60]. Optimum loading of ZnO in the TiO<sub>2</sub>/ZnO composites enhances the generation rate of electron/hole pairs to increase photocatalytic efficiency [61]. Concurrently, it increases the formation of hydroxyl radicals to improve photocatalytic performances [62].

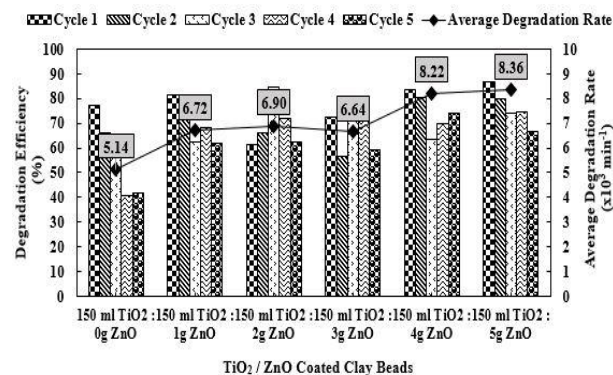


**Figure 5** Recycling of TiO<sub>2</sub>/ZnO-coated clay beads in terms of MB degradation efficiency and average rate constant

## 4.0 CONCLUSION

In this study, Preparation of the TiO<sub>2</sub>/ZnO-coated clay beads was conducted via a sol-gel process using clay beads as substrate, where characterization of the prepared beads was done via SEM and EDS. The results demonstrate that coated clay beads were composed of nanoparticles. Small agglomerates are dispersed homogeneously in the TiO<sub>2</sub>/5 g ZnO-coated clay beads. An optimal TiO<sub>2</sub>/ZnO ratio of TiO<sub>2</sub>/5 g ZnO was found to achieve a higher degradation efficiency with a  $k$ -value of 0.00836 min<sup>-1</sup>. Furthermore, the immobilized TiO<sub>2</sub>/ZnO recyclability over clay beads up to five cycles without any catalyst reactivation proves the acceptability of clay beads in photocatalytic treatment. In the future, more studies and research on catalyst immobilization of LECA clay beads remain necessary to upgrade the photocatalytic activity. Furthermore, researchers should further investigate the benchmark for raw chemicals used to prepare synthesis sol-gel since every ratio will give different results. This application will help convert lab-scale practices into pilot scales in the industrial plant.

## Acknowledgement

This research was funded by Talent and Publication Enhancement-Research Grant (TAPE-RG) and internal funding from Universiti Malaysia Terengganu (grant number 55179 and 55247). The authors gratefully acknowledge Universiti Malaysia Terengganu for the financial support given and the Faculty of Ocean Engineering Technology and

Informatics, Universiti Malaysia Terengganu, for other related contributions.

## References

- [1] Jedla, M. R., B. Koneru, A. Franco, D. Rangappa, and P. Banerjee. 2022. Recent Developments in Nanomaterials-based Adsorbents for Water Purification Techniques. *Biointerface Res. Appl. Chem.* 12: 5821-5835. DOI: <https://doi.org/10.33263/BRIAC125.58215835>.
- [2] Ambigadevi, J., P. Senthil Kumar, D. V. N. Vo, S. Hari Haran, and T. N. Srinivasa Raghavan. 2021. Recent Developments in Photocatalytic Remediation of Textile Effluent using Semiconductor based Nanostructured Catalyst: A Review. *Journal of Environmental Chemical Engineering.* 9(11). DOI: <https://doi.org/10.1016/j.jece.2020.104881>.
- [3] Dorian, A. H. H., and C. C. Sorrell. 2011. Review of the Anatase to Rutile Phase Transformation. *J. Mater. Sci.* 46: 855-874. DOI: <https://doi.org/10.1007/s10853-010-5113-0>.
- [4] Hassan, M.bE., J. Chen, G. Liu, D. Zhu, and J. Cai. 2014. Enhanced Photocatalytic Degradation of Methyl Orange Dye under the Daylight Irradiation over CN-TiO<sub>2</sub> Modified with OMS-2. *Materials.* 7(12): 8024-8036. DOI: <https://doi.org/10.3390/ma7128024>.
- [5] Mammadov, G. S., M. A. Ramazanov, A. Kanaev, U. A. Hasanova, and K. A. Huseynov. 2017. Photocatalytic Degradation of Organic Pollutants in Air by Application of Titanium Dioxide Nanoparticles. *Chem. Eng. Trans.* 60: 241-246. DOI: <https://doi.org/10.3303/CET1760041>.
- [6] Hachem, C., Bocquillon, F., Zahraa, O., and Bouchy, M. 2001. Decolorization of Textile Industry Wastewater by the Photocatalytic Degradation Process. *Dyes and Pigments.* 49(2): 117-125. DOI: [https://doi.org/10.1016/S0143-7208\(01\)00014-6](https://doi.org/10.1016/S0143-7208(01)00014-6).
- [7] Hamed, N. K. A., Ahmad, M. K., Hairom, N. H. H., Faridah, A. B., Mamat, M. H., Mohamed, A., and Shimomura, M. 2022. Photocatalytic Degradation of Methylene Blue by Flowerlike Rutile-phase TiO<sub>2</sub> Film Grown via Hydrothermal Method. *Journal of Sol-Gel Science and Technology.* 102(3): 637-648. DOI: <https://doi.org/10.1007/s10971-021-05691-y>.
- [8] Kanakaraju, D., S. Ravichandar, and Y. C. Lim. 2017. Combined Effects of Adsorption and Photocatalysis by Hybrid TiO<sub>2</sub>/ZnO-calcium Alginate Beads for the Removal of Copper. *J. Environ. Sci. (China).* 55: 214-223. DOI: <https://doi.org/10.1016/j.jes.2016.05.043>.
- [9] Mansilla, H. D., Villaseñor, J., Maturana, G., Baeza, J., Freer, J., and Durán, N. 1994. ZnO-catalysed Photodegradation of Kraft Black Liquor. *Journal of Photochemistry and Photobiology, A: Chemistry.* 78(3): 267-273. DOI: [https://doi.org/10.1016/1010-6030\(93\)03731-U](https://doi.org/10.1016/1010-6030(93)03731-U).
- [10] Al-Hasani, H., Al-Sabahi, J., Al-Ghafri, B., Al-Hajri, R., and Al-Abri, M. 2022. Effect of Water Quality in Photocatalytic Degradation of Phenol using Zinc Oxide Nanorods under Visible Light Irradiation. *Journal of Water Process Engineering.* 49. DOI: <https://doi.org/10.1016/j.jwpe.2022.103121>.
- [11] Dimapilis, E. A. S., C. S. Hsu, R. M. O. Mendoza, and M. C. Lu. 2018. Zinc Oxide Nanoparticles for Water Disinfection. *Sustain. Environ. Res.* 28: 47-56. DOI: <https://doi.org/10.1016/j.serj.2017.10.001>.
- [12] Javed, A. H., N. Shahzad, M. A. Khan, M. Ayub, N. Iqbal, M. Hassan, and M. I. Shahzad. 2021. Effect of ZnO Nanostructures on the Performance of Dye Sensitized Solar Cells. *Solar Energy.* 230: 492-500. DOI: <https://doi.org/10.1016/j.solener.2021.10.045>.
- [13] Das, A., P. M. Kumar, M. Bhagavathiachari, and R. G. Nair. 2020. Hierarchical ZnO-TiO<sub>2</sub> Nanoheterojunction: A Strategy Driven Approach to Boost the Photocatalytic Performance through the Synergy of Improved Surface Area and Interfacial Charge Transport. *Appl. Surf. Sci.* 534. DOI: <https://doi.org/10.1016/j.apsusc.2020.147321>.
- [14] Bai, N., X. Liu, Z. Li, X. Ke, K. Zhang, and Q. Wu. 2021. High-efficiency TiO<sub>2</sub>/ZnO Nanocomposites Photocatalysts by Sol-gel and Hydrothermal Methods. *Journal of Sol-Gel Science and Technology.* 99(1): 92-100. DOI: <https://doi.org/10.1007/s10971-021-05552-8>.
- [15] Ong, C. B., L. Y. Ng, and A. W. Mohammad. 2018. A Review of ZnO Nanoparticles as Solar Photocatalysts: Synthesis, Mechanisms and Applications. *Renew. Sust. Energ. Rev.* 81: 536-551. DOI: <https://doi.org/10.1016/j.rser.2017.08.020>.
- [16] Shayegan, Z., C. S. Lee, and F. Haghghat. 2018. TiO<sub>2</sub> Photocatalyst for Removal of Volatile Organic Compounds in Gas Phase – A Review. *Chem. Eng. J.* 334: 2408-2439. DOI: <https://doi.org/10.1016/j.cej.2017.09.153>.
- [17] Kurian, M. 2021. Advanced Oxidation Processes and Nanomaterials. A Review. *Cleaner Engineering and Technology.* 2. DOI: <https://doi.org/10.1016/j.clet.2021.100090>.
- [18] Xu, X., J. Wang, J. Tian, X. Wang, J. Dai, and X. Liu. 2011. Hydrothermal and Post-heat Treatments of TiO<sub>2</sub>/ZnO Composite Powder and Its Photodegradation Behavior on Methyl Orange. *Ceram. Int.* 37(7): 2201-2206. DOI: <https://doi.org/10.1016/j.ceramint.2011.03.067>.
- [19] Liao, M. H., C. H. Hsu, and D. H. Chen. 2006. Preparation and Properties of Amorphous Titania-coated Zinc Oxide Nanoparticles. *J. Solid State Chem.* 179(7): 2020-2026. DOI: <https://doi.org/10.1016/j.jssc.2006.03.042>.
- [20] Arunachalam, A., S. Dhanapandian, C. Manoharan, and G. Sivakumar. 2015. Physical Properties of Zn Doped TiO<sub>2</sub> Thin Films with Spray Pyrolysis Technique and Its Effects in Antibacterial Activity. *Spectrochim. Acta - Part A: Mol. Biomol. Spectrosc.* 138: 105-112. DOI: <https://doi.org/10.1016/j.saa.2014.11.016>.
- [21] Eadi, S.B., T. T. Duong, and S. Kim. 2018. TiO<sub>2</sub> Coated ZnO Nanorods Growth using NCD Process and their Gas Sensing Properties. *Superlattices Microst.* 120: 250-256. DOI: <https://doi.org/10.1016/j.spmi.2018.03.021>.
- [22] Özdokur, K. V., B. B. Çırak, B. Çağlar, C. Çırak, S. M. Kradeniz, T. Kılınc, and A. E. Ekinci. 2018. Fabrication of TiO<sub>2</sub>/ZnO/Pt Nanocomposite Electrode with Enhanced Electrocatalytic Activity for Methanol Oxidation. *Vacuum* 155: 242-248. DOI: <https://doi.org/10.1016/j.vacuum.2018.06.024>.
- [23] Deebansok, S., T. Amornsakchai, P. Sae-Ear, P. Siriphannon, and S. M. Smith. 2021. Sphere-like and Flake-like ZnO Immobilized on Pineapple Leaf Fibers as Easy-to-recover Photocatalyst for the Degradation of Congo Red. *Journal of Environmental Chemical Engineering.* 9(2). DOI: <https://doi.org/10.1016/j.jece.2020.104746>.
- [24] Pérez-González, M., S. A. Tomás, J. Santoyo-Salazar, and M. Morales-Luna. 2017. Enhanced Photocatalytic Activity of TiO<sub>2</sub>-ZnO Thin Films Deposited by dc Reactive Magnetron Sputtering. *Ceram. Int.* 43(12): 8831-8838. DOI: <https://doi.org/10.1016/j.ceramint.2017.04.016>.
- [25] Hakkı, H. K., S. Allahyari, N. Rahemi, and M. Tasbihi. 2019. Surface Properties, Adherence, and Photocatalytic Activity of Sol-gel Dip-coated TiO<sub>2</sub>-ZnO Films on Glass Plates. *Comptes Rendus Chimie.* 22(5): 393-405. DOI: <https://doi.org/10.1016/j.crci.2019.05.007>.
- [26] Ali, M. M., Md. J. Haque, M. H. Kabir, M. A. Kaiyum, and M. S. Rahman. 2021. Nano Synthesis of ZnO-TiO<sub>2</sub> Composites by Sol-gel Method and Evaluation of Their Antibacterial, Optical and Photocatalytic Activities. *Results in Materials.* 11: 100-199. DOI: <https://doi.org/10.1016/j.rinma.2021.100199>.
- [27] Sethi, D., and R. Sakthivel. 2017. ZnO/TiO<sub>2</sub> Composites for Photocatalytic Inactivation of Escherichia coli. *J. Photochem. Photobiol. B: Biol.* 168: 117-123. DOI: <https://doi.org/10.1016/j.jphotobiol.2017.02.005>.

- [28] Tseng, T. K., Y. S. Lin, Y. J. Chen, and H. Chu. 2010. A Review of Photocatalysts Prepared by Sol-gel Method for VOCs Removal. *Int. J. Mol. Sci.* 11: 2336-2361. DOI: <https://doi.org/10.3390/ijms11062336>.
- [29] Mustapha, S., M. M. Ndamiiso, A. S. Abdulkareem, J. O. Tijani, D. T. Shuaib, A. O. Ajala, and A. K. Mohammed. 2020. Application of TiO<sub>2</sub> and ZnO Nanoparticles Immobilized on Clay in Wastewater Treatment: A Review. *Appl. Water Sci.* 10(1). DOI: <https://doi.org/10.1007/s13201-019-1138-y>.
- [30] Parashar, M., V. K. Shukla, and R. Singh. 2020. Metal Oxides Nanoparticles via Sol-gel Method: A Review on Synthesis, Characterization and Applications. *J. Mater. Sci.: Mater. Electron.* 31: 3729-3749. DOI: <https://doi.org/10.1007/s10854-020-02994-8>.
- [31] Ceretta, M. B., Y. Vieira, E. A. Wolski, E. L. Foletto, and S. Silvestri. 2020. Biological Degradation Coupled to Photocatalysis by ZnO/polypyrrole Composite for the Treatment of Real Textile Wastewater. *J. Water Process. Eng.* 35: 101230. DOI: <https://doi.org/10.1016/j.jwpe.2020.101230>.
- [32] Danfá, S., R. C. Martins, M. J. Quina, and J. Gomes. 2021. Supported TiO<sub>2</sub> in Ceramic Materials for the Photocatalytic Degradation of Contaminants of Emerging Concern in Liquid Effluents: A Review. *Molecules.* 26: 5363. DOI: <https://doi.org/10.3390/molecules26175363>.
- [33] Tekin, D., H. Kiziltas, and H. Ungan. 2020. Kinetic Evaluation of ZnO/TiO<sub>2</sub> Thin Film Photocatalyst in Photocatalytic Degradation of Orange G. *J. Mol. Liq.* 306. DOI: <https://doi.org/10.1016/j.molliq.2020.112905>.
- [34] Munguti, K. L., and D. F. Birhanu. 2021. High Photodegradation Performance of ZnO Nanoparticles Supported on Porous Zeolite Na-a: Effects of ZnO Loading. *Research Square*. DOI: <http://dx.doi.org/10.21203/rs.3.rs-430420/v1>.
- [35] Anusuya, N., C. Pragathiswaran, and J. V. Mary. 2021. A Potential Catalyst - TiO<sub>2</sub>/ZnO based Chitosan Gel Beads for the Reduction of Nitro-aromatic Compounds Aggregated Sodium Borohydride and their Antimicrobial Activity. *J. Mol. Struct.* 1236: 130197. DOI: <https://doi.org/10.1016/j.molstruc.2021.130197>.
- [36] Elkholy, R. A., E. M. Khalil, A. B. Farag, M. M. Abo El-Fadl, and A. M. El-Aassar. 2020. Photocatalytic Degradation of Organic Pollutants in Wastewater using Different Nanomaterials Immobilized on Polymeric Beads. *Desalin. Water Treat.* 193: 117-128. DOI: <https://doi.org/10.5004/dwt.2020.25680>.
- [37] Kaur, T., A. Sraw, R. K. Wanchoo, and A. P. Toor. 2018. Solar Assisted Degradation of Carbendazim in Water Using Clay Beads Immobilised with TiO<sub>2</sub> & Fe doped TiO<sub>2</sub>. *Sol. Energy.* 162: 45-56. DOI: <https://doi.org/10.1016/j.solener.2017.11.033>.
- [38] Bel Hadjitaief, H., Ben Zina, M., Galvez, M. E., and Da Costa, P. 2016. Photocatalytic Degradation of Methyl Green Dye in Aqueous Solution over Natural Clay-supported ZnO-TiO<sub>2</sub> Catalysts. *Journal of Photochemistry and Photobiology A: Chemistry.* 315: 25-33. DOI: <https://doi.org/10.1016/j.jphotochem.2015.09.008>.
- [39] Vaizogullar, A. I. 2017. TiO<sub>2</sub>/ZnO Supported on Sepiolite: Preparation, Structural Characterization, and Photocatalytic Degradation of Flumequine Antibiotic in Aqueous Solution. *Chemical Engineering Communications.* 204(6): 689-697. DOI: <https://doi.org/10.1080/00986445.2017.1306518>.
- [40] Wang, H., Zhou, P., Wang, J., Wang, Y., Wei, J., Zhan, H., and Zhang, Y. 2018. Synthesis and Characterization of Rectorite/ZnO/TiO<sub>2</sub> Composites and Their Properties of Adsorption and Photocatalysis for the Removal of Methylene Blue Dye. *Journal Wuhan University of Technology, Materials Science Edition.* 33(3): 729-735. DOI: <https://doi.org/10.1007/s11595-018-1885-x>.
- [41] Son, B. T., N. V. Long, and N. T. Nhat Hang. 2021. Fly ash-, foundry Sand-, Clay-, and Pumice-based Metal Oxide Nanocomposites as Green Photocatalysts. *RSC Advances. Royal Society of Chemistry.* 11: 30805-30826. DOI: <https://doi.org/10.1039/d1ra05647f>.
- [42] Unuabonah, E. I., C. G. Ugwuja, M. O. Omorogie, A. Adewuyi, and N. A. Oladoja. 2018. Clays for Efficient Disinfection of Bacteria in Water. *Appl. Clay Sci.* 151: 211-223. DOI: <https://doi.org/10.1016/j.clay.2017.10.005>.
- [43] Ouda, A. S., and A. M. Rashad. 2021. An Investigation on the Performance of Lightweight Mortar-based Geopolymer Containing High-volume LECA Aggregate against High Temperatures. *Environmental Science and Pollution Research.* DOI: <https://doi.org/10.1007/s11356-021-17819-2>.
- [44] Revellame, E. D., D. L. Fortela, W. Sharp, R. Hernandez, and M. E. Zappi. 2020. Adsorption Kinetic Modeling using Pseudo-first Order and Pseudo-second order Rate Laws: A Review. *Cleaner Engineering and Technology.* 1. DOI: <https://doi.org/10.1016/j.clet.2020.100032>.
- [45] Hosseini, A., H. Karimi, J. Foroughi, M. M. Sabzehmeidani, and M. Ghaedi. 2021. Heterogeneous Photoelectro-Fenton using ZnO and TiO<sub>2</sub> Thin Film as Photocatalyst for Photocatalytic Degradation Malachite Green. *Applied Surface Science Advances.* 6. DOI: <https://doi.org/10.1016/j.apsadv.2021.100126>.
- [46] Isik, Z., Z. Bilici, S. K. Adiguzel, H. C. Yatmaz, and N. Dizge. 2019. Entrapment of TiO<sub>2</sub> and ZnO Powders in Alginate Beads: Photocatalytic and Reuse Efficiencies for Dye Solutions and Toxicity Effect for DNA Damage. *Environ. Technol. Innov.* 14. DOI: <https://doi.org/10.1016/j.eti.2019.100358>.
- [47] Bai, Q., M. Lavenas, L. Vauriot, Q. Le Tréquesser, J. Hao, F. Weill, and M. H. Delville. 2019. Hydrothermal Transformation of Titanate Scrolled Nanosheets to Anatase over a Wide pH Range and Contribution of Triethanolamine and Oleic Acid to Control the Morphology. *Inorg. Chem.* 58(4): 2588-2598. DOI: <https://doi.org/10.1021/acs.inorgchem.8b03197>.
- [48] David, M. E., R. M. Ion, R. M. Grigorescu, L. Iancu, and E. R. Andrei. 2020. Nanomaterials used in Conservation and Restoration of Cultural Heritage: An up-to-date Overview. *Mater.* 13(9). DOI: <https://doi.org/10.3390/ma13092064>.
- [49] Liao, D. L., C. A. Badour, and B. Q. Liao. 2008. Preparation of Nanosized TiO<sub>2</sub>/ZnO Composite Catalyst and its Photocatalytic Activity for Degradation of Methyl Orange. *J. Photochem. Photobiol. A: Chem.* 194(1): 11-19. DOI: <https://doi.org/10.1016/j.jphotochem.2007.07.008>.
- [50] Jiang, Q., Z. Han, Y. Yuan, C. Cai, J. Li, and Z. Cheng. 2022. Controlled Preparation and Photocatalytic Performance of TiO<sub>2</sub>/ZnO Phase-mixed Nanotubes-based Nano-spheres. *Materials Chemistry and Physics.* 279. DOI: <https://doi.org/10.1016/j.matchemphys.2022.125737>.
- [51] Mousa, H. M., J. F. Alenezi, I. M. A. Mohamed, A. S. Yasin, A. F. M. Hashem, and A. Abdal-hay. 2021. Synthesis of TiO<sub>2</sub>@ZnO Heterojunction for Dye Photodegradation and Wastewater Treatment. *J. Alloys Compd.* 886. DOI: <https://doi.org/10.1016/j.jallcom.2021.161169>.
- [52] Munguti, L., and F. Dejene. 2021. Effects of Zn: Ti Molar Ratios on the Morphological, Optical and Photocatalytic Properties of ZnO-TiO<sub>2</sub> Nanocomposites for Application in Dye Removal. *Mater. Sci. Semicon. Process.* 128. DOI: <https://doi.org/10.1016/j.mssp.2021.105786>.
- [53] De Jong, T. A., D. N. L. Kok, A. J. H. van der Torren, H. Schopmans, R. M. Tromp, S. J. van der Molen, and J. Jobst. 2020. Quantitative Analysis of Spectroscopic Low Energy Electron Microscopy Data: High-dynamic Range Imaging, Drift Correction and Cluster Analysis. *Ultramicroscopy.* 213. DOI: <https://doi.org/10.1016/j.ultramic.2019.112913>.
- [54] Prasannalakshmi, P., and N. Shanmugam. 2017. Fabrication of TiO<sub>2</sub>/ZnO Nanocomposites for Solar Energy Driven Photocatalysis. *Mater. Sci. Semicon. Process.* 61: 114-124. DOI: <https://doi.org/10.1016/j.mssp.2017.01.008>.



- [55] Moradi, S., P. Aberoomand-Azar, S. Raeis-Farshid, S. Abedini-Khorrami, and M. H. Givianrad. 2016. The Effect of Different Molar Ratios of ZnO on Characterization and Photocatalytic Activity of TiO<sub>2</sub>/ZnO Nanocomposite. *J. Saudi Chem. Soc.* 20(4): 373-378. DOI: <https://doi.org/10.1016/j.jscs.2012.08.002>.
- [56] Siwińska-Stefańska, K., A. Kubiak, A. Piasecki, J. Goscińska, G. Nowaczyk, S. Jurga, and T. Jesionowski. 2018. TiO<sub>2</sub>-ZnO Binary Oxide Systems: Comprehensive Characterization and Tests of Photocatalytic Activity. *Materials.* 11(5). DOI: <https://doi.org/10.3390/ma11050841>.
- [57] Zheng, X., D. Zhang, Y. Gao, Y. Wu, Q. Liu, and X. Zhu. 2019. Synthesis and Characterization of Cubic Ag/TiO<sub>2</sub> Nanocomposites for the Photocatalytic Degradation of Methyl Orange in Aqueous Solutions. *Inorg. Chem. Commun.* 110. DOI: <https://doi.org/10.1016/j.inoche.2019.107589>.
- [58] Azfar, A. K., M. F. Kasim, I. M. Lokman, H. A. Rafeie, and M. S. Mastuli. 2020. Comparative Study on Photocatalytic Activity of Transition Metals (Ag and Ni)doped ZnO Nanomaterials Synthesized via Sol-gel Method. *R. Soc. Open Sci.* 7(2). DOI: <https://doi.org/10.1098/rsos.191590>.
- [59] Do, J. Y., R. K. Chava, K. K. Mandari, N. K. Park, H. J. Ryu, M. W. Seo, and M. Kang. 2018. Selective Methane Production from Visible-light-driven Photocatalytic Carbon Dioxide Reduction using the Surface Plasmon Resonance Effect of Superfine Silver Nanoparticles Anchored on Lithium Titanium Dioxide Nanocubes (Ag@LiTiO<sub>2</sub>). *Appl. Catal. B: Environ.* 237: 895-910. DOI: <https://doi.org/10.1016/j.apcatb.2018.06.070>.
- [60] Deng, W., Q. Dai, Y. Lao, B. Shi, and X. Wang. 2016. Low Temperature Catalytic Combustion of 1,2-dichlorobenzene over CeO<sub>2</sub>-TiO<sub>2</sub> Mixed Oxide Catalysts. *Appl. Catal. B: Environ.* 181: 848-861. DOI: <https://doi.org/10.1016/j.apcatb.2015.07.053>.
- [61] Liu, R., H. Ye, X. Xiong, and H. Liu. 2010. Fabrication of TiO<sub>2</sub>/ZnO Composite Nanofibers by Electrospinning and Their Photocatalytic Property. *Mater. Chem. Phys.* 121(3): 432-439. DOI: <https://doi.org/10.1016/j.matchemphys.2010.02.002>.
- [62] El-Naggar, M. E., A. R. Wassel, and K. Shoueir. 2021. Visible-light Driven Photocatalytic Effectiveness for Solid-state synthesis of ZnO/natural clay/TiO<sub>2</sub> Nanoarchitectures Towards Complete Decolorization of Methylene Blue from Aqueous Solution. *Environ. Nanotechnol. Monit. Manag.* 15. DOI: <https://doi.org/10.1016/j.enmm.2020.100425>.